Leptogenesis and dark matter from a low scale seesaw mechanism

Ang Liu, Zhi-Long Han,[*] Yi Jin, and Fa-Xin Yang

School of Physics and Technology, University of Jinan, Jinan, Shandong 250022, China

In this paper, we perform a detailed analysis of the phenomenology of leptogenesis and dark matter from a low scale seesaw mechanism. In the framework of Neutrinophilic two Higgs doublet model, we further introduce one scalar singlet ϕ and one Dirac fermion singlet χ, which are charged under a Z_2 symmetry. Assuming the coupling of χ is extremely small, it serves as feebly interacting massive particle (FIMP) dark matter. Heavy right-hand neutrinos N provide a common origin for tiny neutrino mass (via a seesaw mechanism), leptogenesis (via $N \to \ell_L \Phi_\nu^*, \bar{\ell}_L \Phi_\nu$), and dark matter (via $N \to \chi\phi$). With hierarchical right-hand neutrino masses, the explicit calculation shows that successful thermal leptogenesis is viable even for TeV-scale N_1 with 0.4 GeV $\lesssim v_\nu \lesssim$ 1 GeV and lightest neutrino mass $m_1 \lesssim 10^{-11}$ eV. In such a scenario, light FIMP dark matter in the keV to MeV range is naturally expected. The common parameter space for neutrino mass, natural leptogenesis, and FIMP dark matter is also obtained in this paper.

I. INTRODUCTION

Besides the success of the standard model (SM), there are still several open questions. In particular, the tiny neutrino mass, baryon asymmetry of the Universe (BAU), and dark matter (DM) are the three outstanding pieces of evidence that require physics beyond the SM. The discovery of neutrino oscillations [1,2] indicates that the masses of neutrinos are at the sub-eV scale, which is at least 6 orders of magnitude smaller than the charged leptons. Known as the type-I seesaw mechanism [3,4], this extensively considered way to naturally incorporate neutrino masses is via introducing three right-hand neutrinos N together with high scale Majorana masses of N,

$$-\mathcal{L}_Y \supset y\bar{L}\tilde{\Phi}N + \frac{1}{2}\bar{N}^c m_N N + \text{H.c.}, \qquad (1)$$

where Φ is the SM Higgs doublet. After spontaneous electroweak symmetry breaking, neutrinos achieve masses as

$$m_\nu = -\frac{v^2}{2}y m_N^{-1} y^T. \qquad (2)$$

Typically, $m_\nu \sim \mathcal{O}(0.1)$ eV is obtained with $y \sim \mathcal{O}(1)$ and $m_N \sim \mathcal{O}(10^{14})$ GeV. Meanwhile, the heavy neutrino can also account for BAU via leptogenesis [5]. For canonical thermal leptogenesis with hierarchal right-hand neutrinos, an upper limit on the charge-parity (CP) asymmetry exists; thus, a lower limit on the mass of lightest right-hand neutrino M_1 should be satisfied [6],

$$M_1 \gtrsim 5 \times 10^8 \text{ GeV} \left(\frac{v}{246 \text{ GeV}}\right)^2. \qquad (3)$$

Therefore, both tiny neutrino mass and leptogenesis favor the high scale N in the type-I seesaw mechanism. However, for such a high scale N, a naturalness problem might arise [7]. By requiring radiative corrections to the $m_\Phi^2 \Phi^\dagger \Phi$ term no larger than 1 TeV^2, it is found that [8]

$$M_1 \lesssim 3 \times 10^7 \text{ GeV} \left(\frac{v}{246 \text{ GeV}}\right)^{2/3} \qquad (4)$$

should be satisfied. It is clear that naturalness is incompatible with canonical leptogenesis. One viable pathway to overcome this is lowering the leptogenesis scale by imposing resonant leptogenesis [9], an Akhmedov-Rubakov-Smirnov mechanism via neutrino oscillation [10,11], or Higgs decay [12,13]. The success of these scenarios depends on the degenerate mass of right-hand neutrinos [14,15], which seems is another sense of unnaturalness. An alternative scenario with hierarchal right-hand neutrinos is employing an intrinsic low scale neutrino mass model, e.g., Neutrinophilic two Higgs doublet model (ν2HDM) [16,17] or Scotogenic model [18–26]. In this paper, we consider ν2HDM [27]. Based on the previous brief discussion in Refs. [17,28,29], we perform a detailed analysis of leptogenesis, especially focusing on dealing with the corresponding Boltzmann equations to obtain the viable parameter space.

*sps_hanzl@ujn.edu.cn

On the other hand, dark matter accounts for more than 5 times the proportion of visible baryonic matter in our current cosmic material field. In principle, one can regard the lightest right-hand neutrino N_1 at the keV scale as sterile neutrino DM [30–33]. However, various constraints leave a quite small viable parameter space [34]. Meanwhile, leptogenesis with two hierarchal right-hand neutrinos is still at high scale [23,35,36]. In this paper, we further introduce a dark sector with one scalar singlet ϕ and one Dirac fermion singlet χ, which are charged under a Z_2 symmetry [37,38]. Stability of DM χ is protected by the Z_2 symmetry; therefore, the stringent x-ray limits can be avoided [34]. In light of the null results from DM direct detection [39] and indirect detection [40], we consider χ as feebly interacting massive particle (FIMP) DM [41].

The structure of the paper is as follows. In Sec. II, we briefly introduce our model. Leptogenesis with hierarchal right-hand neutrinos is discussed in Sec. III. The relic abundance of FIMP DM χ and constraint of free-streaming length are considered in Sec. IV. Viable parameter space for leptogenesis and DM is obtained by a random scan in Sec. V. We conclude our work in Sec. VI.

II. THE MODEL

The original TeV-scale ν2HDM for neutrino mass was proposed in Ref. [27]. The model is extended by one neutrinophilic scalar doublet Φ_ν with the same quantum numbers as the SM Higgs doublet Φ and three right-hand heavy neutrinos N. To forbid the direct type-I seesaw interaction $\bar{L}\tilde{\Phi}N$, a global $U(1)_L$ symmetry should be employed, under which $L_\Phi = 0$, $L_{\Phi_\nu} = -1$, and $L_N = 0$. Therefore, Φ_ν will specifically couple to N, and Φ will couple to quarks and charged leptons as in the SM. For the dark sector, one scalar singlet ϕ and one Dirac fermion singlet χ are further introduced, which are charged under a Z_2 symmetry. Provided $m_\chi < m_\phi$, then χ serves as a DM candidate.

The scalar doublets could be denoted as

$$\Phi = \begin{pmatrix} \phi^+ \\ \frac{v+\phi^{0,r}+i\phi^{0,i}}{\sqrt{2}} \end{pmatrix}, \qquad \Phi_\nu = \begin{pmatrix} \phi_\nu^+ \\ \frac{v_\nu+\phi_\nu^{0,r}+i\phi_\nu^{0,i}}{\sqrt{2}} \end{pmatrix}. \quad (5)$$

The corresponding Higgs potential is then

$$V = m_\Phi^2 \Phi^\dagger \Phi + m_{\Phi_\nu}^2 \Phi_\nu^\dagger \Phi_\nu + m_\phi^2 \phi^\dagger \phi + \frac{\lambda_1}{2}(\Phi^\dagger \Phi)^2$$

$$+ \frac{\lambda_2}{2}(\Phi_\nu^\dagger \Phi_\nu)^2 + \lambda_3(\Phi^\dagger \Phi)(\Phi_\nu^\dagger \Phi_\nu) + \lambda_4(\Phi^\dagger \Phi_\nu)(\Phi_\nu^\dagger \Phi)$$

$$- (\mu^2 \Phi^\dagger \Phi_\nu + \text{H.c.}) \quad (6)$$

$$+ \frac{\lambda_5}{2}(\phi^\dagger \phi)^2 + \lambda_6(\phi^\dagger \phi)(\Phi^\dagger \Phi) + \lambda_7(\phi^\dagger \phi)(\Phi_\nu^\dagger \Phi_\nu), \quad (7)$$

where the $U(1)_L$ symmetry is broken explicitly but softly by the μ^2 term. For the unbroken Z_2 symmetry, $\langle \phi \rangle = 0$ should be satisfied. Meanwhile, vacuum expectation values (VEVs) of Higgs doublets in terms of parameters of the Higgs potential can be found by deriving the minimization condition

$$v\left[m_\Phi^2 + \frac{\lambda_1}{2}v^2 + \frac{\lambda_3+\lambda_4}{2}v_\nu^2\right] - \mu^2 v_\nu = 0, \quad (8)$$

$$v_\nu\left[m_{\Phi_\nu}^2 + \frac{\lambda_2}{2}v_\nu^2 + \frac{\lambda_3+\lambda_4}{2}v^2\right] - \mu^2 v = 0. \quad (9)$$

Taking the parameter set

$$m_\Phi^2 < 0, \qquad m_{\Phi_\nu}^2 > 0, \qquad |\mu^2| \ll m_{\Phi_\nu}^2, \quad (10)$$

we can obtain the relations of VEVs as

$$v \simeq \sqrt{\frac{-2m_\Phi^2}{\lambda_1}}, \qquad v_\nu \simeq \frac{\mu^2 v}{m_{\Phi_\nu}^2 + (\lambda_3+\lambda_4)v^2/2}. \quad (11)$$

Typically, $v_\nu \sim 1$ GeV is obtained with $\mu \sim 10$ GeV and $m_{\Phi_\nu} \sim 100$ GeV. Since the μ^2 term is the only source of $U(1)_L$ breaking, radiative corrections to μ^2 are proportional to μ^2 itself and are only logarithmically sensitive to the cutoff [42]. Thus, VEV hierarchy $v_\nu \ll v$ is stable against radiative corrections [43,44].

After spontaneous symmetry breaking, the physical Higgs bosons are given by [45]

$$H^+ = \phi_\nu^+ \cos\beta - \phi^+ \sin\beta, \qquad A = \phi_\nu^{0,i} \cos\beta - \phi^{0,i} \sin\beta, \quad (12)$$

$$H = \phi_\nu^{0,r} \cos\alpha - \phi^{0,r} \sin\alpha, \qquad h = \phi_\nu^{0,r} \cos\alpha + \phi^{0,r} \sin\alpha, \quad (13)$$

where the mixing angles β and α are determined by

$$\tan\beta = \frac{v_\nu}{v}, \qquad \tan 2\alpha \simeq 2\frac{v_\nu}{v}\frac{-\mu^2 + (\lambda_3+\lambda_4)vv_\nu}{-\mu^2 + \lambda_1 vv_\nu}. \quad (14)$$

Neglecting the terms of $\mathcal{O}(v_\nu^2)$ and $\mathcal{O}(\mu^2)$, the masses of the physical Higgs bosons are

$$m_{H^+}^2 \simeq m_{\Phi_\nu}^2 + \frac{1}{2}\lambda_3 v^2, \qquad m_A^2 \simeq m_H^2 \simeq m_{H^+}^2 + \frac{1}{2}\lambda_4 v^2,$$

$$m_h^2 \simeq \lambda_1 v^2. \quad (15)$$

Since the mixing angles are suppressed by the small value of v_ν, h is almost identical to the 125 GeV SM Higgs boson

[46,47]. A degenerate mass spectrum of Φ_ν as $m_{H^+} = m_H = m_A = m_{\Phi_\nu}$ is adopted in our following discussion for simplicity, which is certainly allowed by various constraints [48]. Because of the unbroken Z_2 symmetry, the dark scalar singlet ϕ does not mix with the Higgs doublets.

The new Yukawa interaction and mass terms are

$$-\mathcal{L}_Y \supset y\bar{L}\tilde{\Phi}_\nu N + \lambda\bar{\chi}\phi N + \frac{1}{2}\overline{N^c}m_N N + m_\chi\bar{\chi}\chi + \text{H.c.},$$
(16)

$$U_{\text{PMNS}} = \begin{pmatrix} c_{12}c_{13} & s_{12}c_{13} & s_{13}e^{i\delta} \\ -s_{12}c_{23}-c_{12}s_{23}s_{13}e^{-i\delta} & c_{12}c_{23}-s_{12}s_{23}s_{13}e^{-i\delta} & s_{23}c_{13} \\ s_{12}s_{23}-c_{12}c_{23}s_{13}e^{-i\delta} & -c_{12}s_{23}-s_{12}c_{23}s_{13}e^{-i\delta} & c_{23}c_{13} \end{pmatrix} \times \text{diag}(e^{i\varphi_1/2}, 1, e^{i\varphi_2/2}).$$
(18)

Here, we use abbreviations $c_{ij} = \cos\theta_{ij}$ and $s_{ij} = \sin\theta_{ij}$, δ is the Dirac phase, and φ_1, φ_2 are the two Majorana phases. Because of the smallness of v_ν, TeV-scale m_N could be viable to realize 0.1 eV scale light neutrino masses. Using the Casas-Ibarra parametrization [49,50], the Yukawa matrix y can be expressed in terms of neutrino oscillation parameters

$$y = \frac{\sqrt{2}}{v_\nu}U_{\text{PMNS}}\hat{m}_\nu^{1/2}R(\hat{m}_N)^{1/2},$$
(19)

where R is an orthogonal matrix in general and $\hat{m}_N = \text{diag}(M_1, M_2, M_3)$ is the diagonalizable heavy neutrino mass matrix. In this work, we parametrize matrix R as

$$R = \begin{pmatrix} \cos\omega_{12} & -\sin\omega_{12} & 0 \\ \sin\omega_{12} & \cos\omega_{12} & 0 \\ 0 & 0 & 1 \end{pmatrix} \begin{pmatrix} \cos\omega_{13} & 0 & -\sin\omega_{13} \\ 0 & 1 & 0 \\ \sin\omega_{13} & 0 & \cos\omega_{13} \end{pmatrix}$$
$$\times \begin{pmatrix} 1 & 0 & 0 \\ 0 & \cos\omega_{23} & -\sin\omega_{23} \\ 0 & \sin\omega_{23} & \cos\omega_{23} \end{pmatrix},$$
(20)

where $\omega_{12,13,23}$ are arbitrary complex angles.

III. LEPTOGENESIS

Now we consider the leptogenesis of this model. The lepton asymmetry is generated by out-of-equilibrium CP-violating decays of right-hand neutrino $N \to \ell_L\Phi_\nu^*$, $\bar{\ell}_L\Phi_\nu$. Neglecting the flavor effect [51], the CP asymmetry is given by

$$\epsilon_i = \frac{1}{8\pi(y^\dagger y)_{ii}}\sum_{j\neq i}\text{Im}[(y^\dagger y)_{ij}^2]G\left(\frac{M_j^2}{M_i^2},\frac{m_{\Phi_\nu}^2}{M_i^2}\right),$$
(21)

where $\tilde{\Phi}_\nu = i\sigma_2\Phi_\nu^*$. Similar to the canonical type-I seesaw mechanism [3], the mass matrix for light neutrinos can be derived from Eq. (16) as

$$m_\nu = -\frac{v_\nu^2}{2}ym_N^{-1}y^T = U_{\text{PMNS}}\hat{m}_\nu U_{\text{PMNS}}^T,$$
(17)

where $\hat{m}_\nu = \text{diag}(m_1, m_2, m_3)$ is the diagonalizable neutrino mass matrix, and U_{PMNS} is the PMNS (Pontecorvo-Maki-Nakagawa-Sakata) matrix:

where the function $G(x, y)$ is defined as [36]

$$G(x,y) = \sqrt{x}\left[\frac{(1-y)^2}{1-x}+1+\frac{1-2y+x}{(1-y^2)^2}\ln\left(\frac{x-y^2}{1-2y+x}\right)\right].$$
(22)

Using the parametrization of Yukawa coupling y in Eq. (19), it is easy to verify

$$y^\dagger y = \frac{2}{v_\nu^2}\hat{m}_N^{1/2}R^\dagger\hat{m}_\nu R\hat{m}_N^{1/2}.$$
(23)

Hence, the matrix $y^\dagger y$ does not depend on the PMNS matrix, which means that the complex matrix R is the source of CP asymmetry ϵ_i. The asymmetry is dominantly generated by the decay of N_1. Further considering the hierarchal mass spectrum $m_{\Phi_\nu}^2 \ll M_1^2 \ll M_{2,3}^2$, the asymmetry ϵ_1 is simplified to

$$\epsilon_1 \simeq -\frac{3}{16\pi(y^\dagger y)_{11}}\sum_{j=2,3}\text{Im}[(y^\dagger y)_{1j}^2]\frac{M_1}{M_j}.$$
(24)

Similar to the Davidson-Ibarra bound [6], an upper limit on ϵ_1 can be derived

$$|\epsilon_1| \lesssim \frac{3}{16\pi}\frac{M_1 m_3}{v_\nu^2}.$$
(25)

Comparing with the bound in the type-I seesaw mechanism, the asymmetry could be enhanced due to the smallness of VEV v_ν. Therefore, low scale leptogenesis seems to be viable in the ν2HDM [17,28]. Meanwhile, the washout effect is quantified by the decay parameter

$$K = \frac{\Gamma_1}{H(z=1)}, \tag{26}$$

where Γ_1 is the decay width of N_1, H is the Hubble parameter, and $z \equiv M_1/T$ with T being the temperature of the thermal bath. The decay width is given by

$$\Gamma_1 = \frac{M_1}{8\pi}(y^\dagger y)_{11}\left(1 - \frac{m_{\Phi_\nu}^2}{M_1^2}\right)^2, \tag{27}$$

and the Hubble parameter is

$$H = \sqrt{\frac{8\pi^3 g_*}{90}}\frac{T^2}{M_{pl}} = H(z=1)\frac{1}{z^2}, \tag{28}$$

with g_* the effective number of relativistic degrees of freedom and $M_{pl} = 1.2 \times 10^{19}$ GeV. Using Eq. (23), one can verify

$$K \simeq 897\left(\frac{v}{v_\nu}\right)^2\frac{(\hat{m}_\nu^R)_{11}}{\text{eV}}, \tag{29}$$

where $\hat{m}_\nu^R \equiv R^\dagger \hat{m}_\nu R$, and thus,

$$(\hat{m}_\nu^R)_{11} = m_1|\cos\omega_{12}|^2|\cos\omega_{13}|^2 + m_2|\sin\omega_{12}|^2|\cos\omega_{13}|^2$$
$$+ m_3|\sin\omega_{13}|^2. \tag{30}$$

It is obvious that the decay parameter K does not depend on ω_{23}, and it is also enhanced by the smallness of v_ν. Since $(\hat{m}_\nu^R)_{11}$ is typical of the order of $m_3 \sim 0.1$ eV, the decay parameter $K \simeq 5.4 \times 10^6$ when $v_\nu = 1$ GeV. So, even with maximum asymmetry $\epsilon_1^{\max} \sim -6.0 \times 10^{-7}$ for $M_1 = 10^5$ GeV obtained from Eq. (25), a rough estimation of

the final baryon asymmetry gives $Y_{\Delta B} \sim -10^{-3}\epsilon_1^{\max}/K \sim 1.1 \times 10^{-16}$ for strong washout [52], which is far below the currently observed value $Y_{\Delta B}^{\text{obs}} = (8.72 \pm 0.04) \times 10^{-11}$ [53]. Hence, only obtaining an enhanced CP asymmetry ϵ_1 is not enough, one has to deal with the washout effect more carefully.

One promising pathway is to reduce the decay parameter K. For instance, if the weak washout condition $K \lesssim 1$ is realized, then $Y_{\Delta B} \sim -10^{-3}\epsilon_1^{\max} \sim 6.0 \times 10^{-10} > Y_{\Delta B}^{\text{obs}}$. Thus, correct baryon asymmetry can be obtained by slightly tuning ϵ_1. As pointed out in Ref. [23], the small value of K can be realized by choosing small $\omega_{12,13}$. In Fig. 1, we illustrate the dependence of K on lightest neutrino mass m_1 with $v_\nu = 10$ GeV. The left panel shows the special case $\omega_{13} = 0$, where Eq. (30) is simplified to $(\hat{m}_\nu^R)_{11} = m_1|\cos\omega_{12}|^2 + m_2|\sin\omega_{12}|^2 \geq \sqrt{\Delta m_{21}^2}|\sin\omega_{12}|^2$. It is clear that the weak washout condition $K < 1$ favors $|\omega_{12}| \lesssim 10^{-2}$ and $m_1 \lesssim 10^{-6}$ eV. The right panel shows the special case $\omega_{12} = 0$. Similar results are observed in the left panel.

Since the matrix R has no physical meaning, we further consider the resulting Yukawa couplings of N. Then, one can derive an upper bound on the Yukawa couplings of N_1 from the out-of-equilibrium condition $\Gamma_1 < H(z=1)$, i.e.,

$$|y_{i1}|^2 < 4 \times 10^{-17}\frac{M_1}{1\text{ GeV}}. \tag{31}$$

The above tiny Yukawa couplings of N_1 mean that the dominant contributions to neutrino masses are from $N_{2,3}$. To generate neutrino mass $m_3 \gtrsim \sqrt{\Delta m_{\text{atm}}^2} \simeq 0.05$ eV, Eq. (19) implies a lower bound on the Yukawa couplings of $N_{2,3}$,
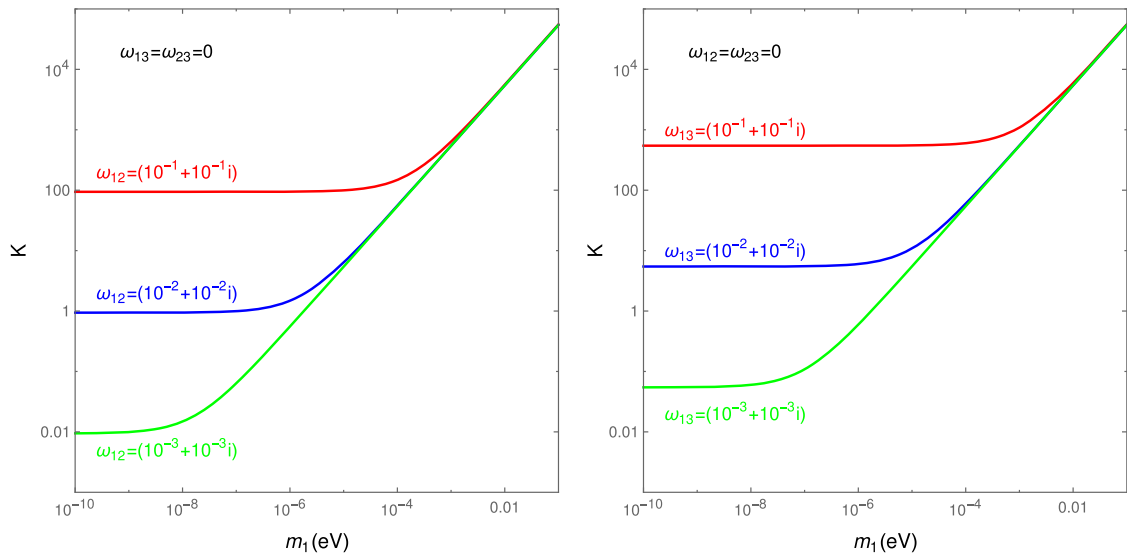

FIG. 1. Decay parameter K as a function of m_1 with $v_\nu = 10$ GeV. Because R must be a complex matrix, we have set $\omega_{ijR} = \omega_{ijI}$.

$$y_{ij} \gtrsim \frac{1 \text{ GeV}}{v_\nu} \sqrt{\frac{M_j}{1 \text{ GeV}}} \times 10^{-5} \quad (j = 2 \text{ or } 3). \quad (32)$$

Therefore, a hierarchical structure of Yukawa coupling y is needed to induce leptogenesis at low scale for the non-degenerate mass of N [19,54]. That is to say, the small value of ω_{12} or ω_{23} of matrix R is to realize such a hierarchical structure of y. One can naturally achieve the suppression of Yukawa coupling y_{i1} by imposing additional symmetry. For instance, a Z_2' symmetry is introduced, under which N_1 and one new scalar singlet ξ are Z_2' odd. Then, an effective interaction $y_\xi \bar{L} \tilde{\Phi}_\nu N_1 \xi / \Lambda$ is obtained, and $y_{i1} = y_\xi \langle \xi \rangle / \Lambda$ is suppressed by the new high energy scale Λ.

On the other hand, the $\Delta L = 2$ washout processes become more significant for small v_ν [17,28]. Notably, for a low scale seesaw mechanism, the narrow width condition $\Gamma_1 / M_1 \ll 1$ is satisfied. Therefore, the evolution of lepton asymmetry and DM abundance actually decouple from each other [55,56]. The evolution of abundance Y_{N_1} and lepton asymmetry $Y_{\Delta L}$ is described by the Boltzmann equations

$$\frac{dY_{N_1}}{dz} = -D(Y_{N_1} - Y_{N_1}^{eq}), \quad (33)$$

$$\frac{dY_{\Delta L}}{dz} = -\epsilon_1 D(Y_{N_1} - Y_{N_1}^{eq}) - W Y_{\Delta L}. \quad (34)$$

The decay term is given by

$$D = Kz \frac{\mathcal{K}_1(z)}{\mathcal{K}_2(z)}. \quad (35)$$

For the washout term, two contributions are considered, i.e., $W = W_{ID} + W_{\Delta L=2}$, where the inverse decay term is

$$W_{ID} = \frac{1}{4} Kz^3 \mathcal{K}_1(z), \quad (36)$$

and the $\Delta L = 2$ scattering term at low temperature is approximately [57]

$$W_{\Delta L=2} \simeq \frac{0.186}{z^2} \left(\frac{246 \text{ GeV}}{v_\nu}\right)^4 \left(\frac{M_1}{10^{10} \text{ GeV}}\right) \left(\frac{\bar{m}}{\text{eV}}\right)^2. \quad (37)$$

Here, $\bar{m}$ is the absolute neutrino mass scale, which is calculated as

$$\bar{m}^2 = m_1^2 + m_2^2 + m_3^2 = 3m_1^2 + \Delta m_{21}^2 + \delta m_{31}^2 \quad (38)$$

for normal hierarchy. According to the latest global fit, we use the best fit values, i.e., $\Delta m_{21}^2 = 7.39 \times 10^{-5} \text{ eV}^2$ and $\delta m_{31}^2 = 2.525 \times 10^{-3} \text{ eV}^2$ [58]. For tiny lightest neutrino mass $m_1 \ll 10^{-2} \text{ eV}$, we actually have $\bar{m} \simeq \sqrt{\delta m_{31}^2} \sim 0.05 \text{ eV}$. Notably, the $\Delta L = 2$ scattering term would be greatly enhanced when $v_\nu \ll v$, so this term is much more important

than it is in vanilla leptogenesis. Then, the sphaleron processes convert the lepton asymmetry into baryon asymmetry as [59]

$$Y_{\Delta B} = \frac{28}{79} Y_{\Delta(B-L)} = -\frac{28}{51} Y_{\Delta L}. \quad (39)$$

Figure 2 shows the washout effect of $\Delta L = 2$ processes. In Fig. 2(a), a weak washout scenario is considered by fixing $K = 10^{-2}$, $|\epsilon_1| = 10^{-6}$, $M_1 = 10^6 \text{ GeV}$ while varying $v_\nu = 10$, $1, 0.1 \text{ GeV}$. It shows that for $v_\nu = 10 \text{ GeV}$, the $\Delta L = 2$ effect is not obvious, but for $v_\nu = 1 \text{ GeV}$, the final baryon asymmetry $Y_{\Delta B}$ is diluted by over 3 orders of magnitude, while for $v_\nu = 0.1 \text{ GeV}$, the $\Delta L = 2$ effect is so strong that the final baryon asymmetry is negligible. The strong washout scenario with $K = 10^2$, $|\epsilon_1| = 10^{-4}$, $M_1 = 10^6 \text{ GeV}$ and varying $v_\nu = 10, 1, 0.1 \text{ GeV}$ is illustrated in Fig. 2(b), where the final baryon asymmetry $Y_{\Delta B}$ for $v_\nu = 1 \text{ GeV}$ is decreased by about 6 orders comparing with the case for $v_\nu = 10 \text{ GeV}$. Therefore, the $\Delta L = 2$ washout effects set a lower bound on v_ν, i.e., $v_\nu \gtrsim 0.3 \text{ GeV}$ as suggested by Ref. [17]. Furthermore, since the $\Delta L = 2$ washout term is also proportional to M_1, the larger M_1 is, the more obvious the washout effect is. The corresponding results are depicted in Fig. 2(c) for the weak washout and Fig. 2(d) for the strong washout. In this way, for a certain value of v_ν, an upper bound on M_1 can be obtained. For instance, when $v_\nu = 1 \text{ GeV}$, then $M_1 \lesssim 10^5 \text{ GeV}$ should be satisfied [28].

IV. DARK MATTER

In our extension of the ν2HDM, the right-hand heavy neutrinos N also couple with fermion singlet χ and scalar singlet ϕ via the Yukawa interaction. The complex Yukawa coupling coefficient λ can lead to CP violation in N decay, and eventually produce asymmetric DM χ [55]. Instead, we consider another interesting scenario, i.e., the FIMP case with the real coupling $\lambda \ll 1$ [56].[1] In this way, the interaction of DM χ is so weak that it never reaches thermalization. Its relic abundance is determined by the freeze-in mechanism [60], which is obtained by solving the following Boltzmann equation

$$\frac{dY_\chi}{dz} = DY_{N_1} \text{BR}_\chi, \quad (40)$$

where BR_χ is the branching ratio of $N_1 \to \chi\phi$. Because of the FIMP nature of χ, the hierarchal condition $\text{BR}_\chi \ll \text{BR}_\ell \simeq 1$ is easily satisfied. The out-of-equilibrium condition for $N_1 \to \chi\phi$ decay is $\Gamma_\chi / H(z = 1) \simeq \text{BR}_\chi \Gamma_1 / H(z = 1) = \text{BR}_\chi K < 1$. In the following studies, we

---

[1]Since Ref. [56] considered canonical leptogenesis with only one scalar doublet, their leptogenesis framework is necessary at high scale. Thus, χ is from high scale N in Ref. [56], and χ is from low scale N in this paper. One can derive that $\lambda \simeq \sqrt{\text{BR}_\chi K M_1} \times 1.2 \times 10^{-8}$. Therefore, the scale of λ in a low scale seesaw mechanism is much smaller than in a canonical seesaw mechanism when BR_χ and K are of the same order.
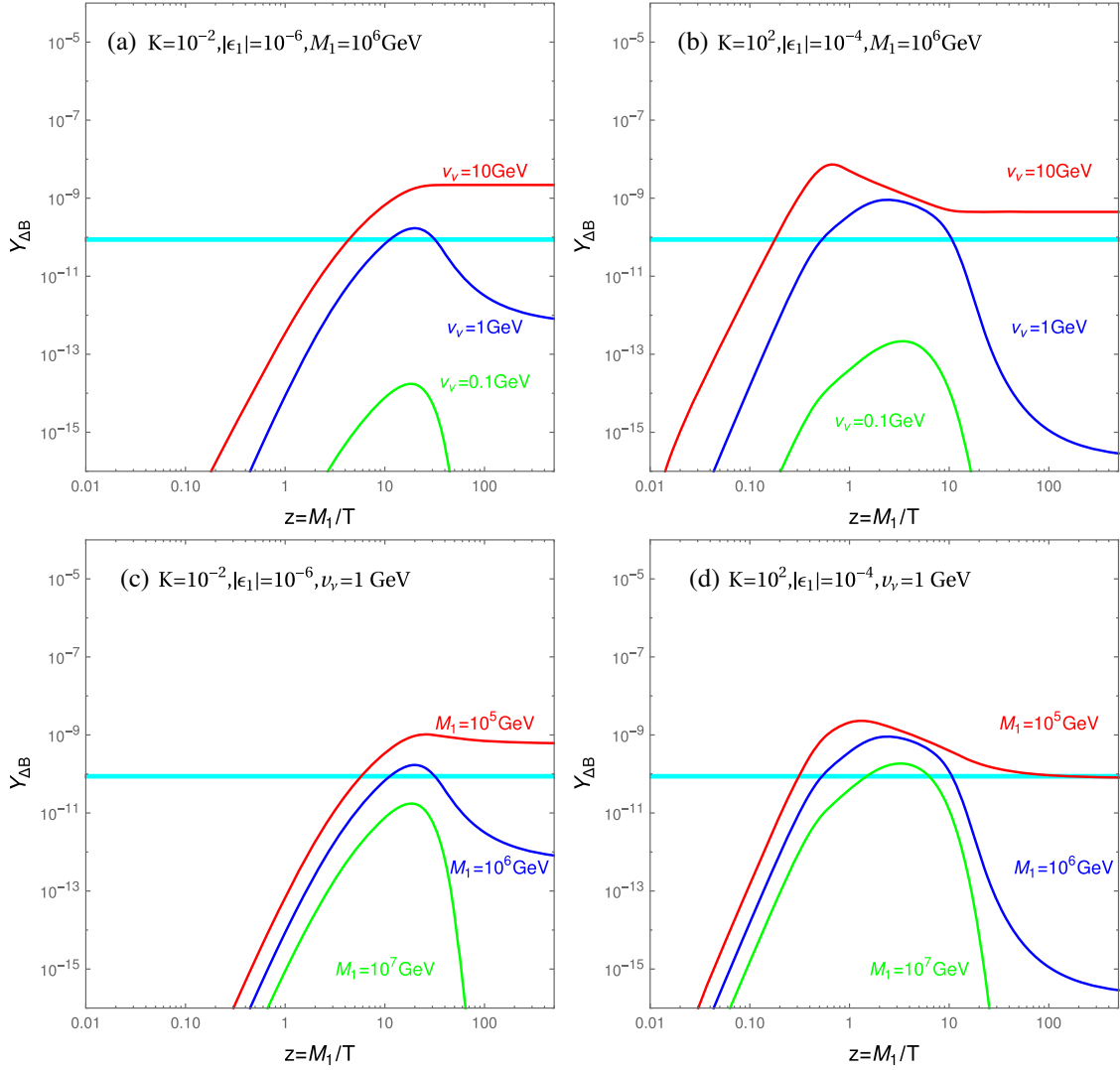
FIG. 2. The washout effect of $\Delta L = 2$ processes. The cyan lines are the observed value $Y_{\Delta B}^{\text{obs}} = 8.72 \times 10^{-11}$. (a) A weak washout scenario with varying v_ν, (b) a strong washout scenario with varying v_ν, (c) a weak washout scenario with varying M_1, and (d) a strong washout scenario with varying M_1.

mainly take $\text{BR}_\chi < 10^{-2}$ and $K \lesssim 10$; thus, the out-of-equilibrium condition is always satisfied. According to the above Boltzmann equation, we can estimate the asymptotic abundance of χ as [56]

$$Y_\chi(\infty) \simeq Y_{N_1}(0)\text{BR}_\chi\left(1 + \frac{15\pi\zeta(5)}{16\zeta(3)}K\right). \quad (41)$$

Then, the corresponding relic abundance is

$$\Omega_\chi h^2 = \frac{m_\chi s_0 Y_\chi(\infty)}{\rho_c}h^2$$

$$\simeq 0.12 \times \left(\frac{m_\chi}{\text{keV}}\right)\left(\frac{\text{BR}_\chi}{10^{-3}}\right)\left(0.009 + \frac{K}{44}\right), \quad (42)$$

where $s_0 = 2891.2\,\text{cm}^{-3}$, $\rho_c = 1.05371 \times 10^{-5}h^2\,\text{GeV}\,\text{cm}^{-3}$ [61]. Typically, the observed relic abundance can be

obtained with $m_\chi \sim 4$ keV, $\text{BR}_\chi \sim 10^{-3}$, and $K \sim 10$. The evolution of DM abundances is shown in Fig. 3. It is clear that when the temperature goes down to $z = m_\chi/T \sim 5$, the abundances Y_χ freeze in and keep at a constant. The left panel of Fig. 3 indicates that m_χ is inversely proportional to BR_χ when the decay parameter K is a constant. For instance, sub-MeV-scale light DM is obtained when $\text{BR}_\chi > 10^{-6}$ with $K = 10$. The right panel of Fig. 3 shows the impact of decay parameter K. Affected by the constant term before K in Eq. (42), we can only conclude that the smaller the K is, the larger the m_χ is. Besides, we also find that the discrepancy between the numerical and analytical results of $Y_\chi(\infty)$ increases when K decreases. Therefore, we adopt the numerical result of $Y_\chi(\infty)$ for a more precise calculation in the following discussion.
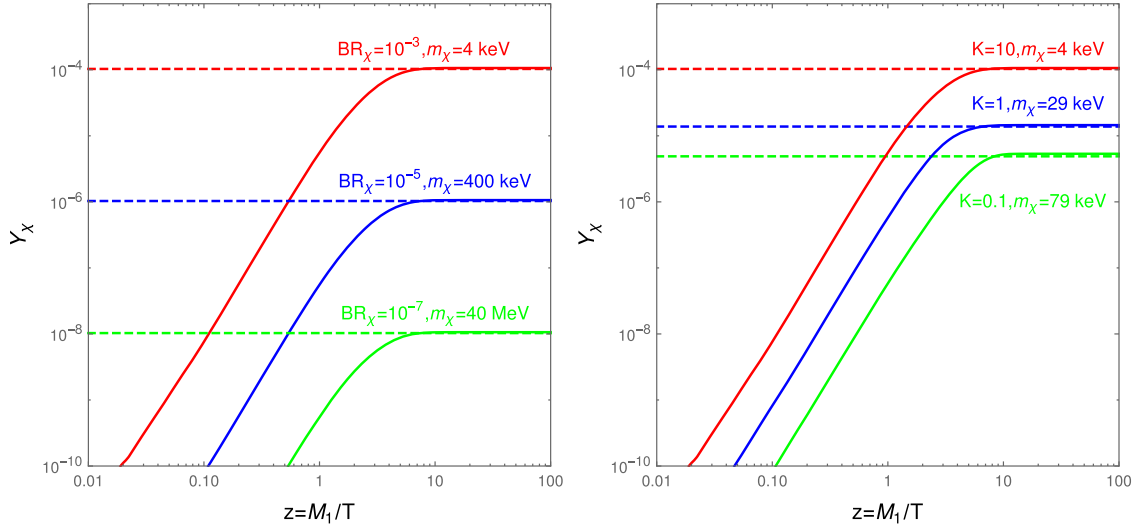
FIG. 3.   Evolution of dark matter abundance with parameter $z = M_1/T$. We fix $K = 10$ in the left panel and $\mathrm{BR}_\chi = 10^{-3}$ in the right panel. The dashed horizontal lines correspond to the estimated results with Eq. (41). DM mass m_χ is obtained by setting $\Omega_\chi h^2 = 0.12$ with the numerical results of $Y_\chi(\infty)$.

The dominant constraint on FIMP DM χ comes from its free-streaming length, which describes the average distance a particle travels without a collision [56]

$$r_{FS} = \int_{a_{rh}}^{a_{eq}} \frac{\langle v \rangle}{a^2 H} da \approx \frac{a_{\mathrm{NR}}}{H_0 \sqrt{\Omega_R}} \left(0.62 + \ln\left(\frac{a_{eq}}{a_{\mathrm{NR}}}\right) \right), \quad (43)$$

where $\langle v \rangle$ is the averaged velocity of DM χ, and a_{eq} and a_{rh} represent scale factors in equilibrium and reheating, respectively. We use the results $H_0 = 67.3\ \mathrm{km\,s^{-1}\,Mpc^{-1}}$, $\Omega_R = 9.3 \times 10^{-5}$, and $a_{eq} = 2.9 \times 10^{-4}$ obtained from Ref. [62]. The nonrelativistic scale factor for FIMP DM is

$$a_{\mathrm{NR}} = \frac{T_0}{2m_\chi} \left(\frac{g_{*,0}}{g_{*,rh}} \right)^{\frac{1}{3}} K^{-\frac{1}{2}}. \quad (44)$$

Taking $g_{*,0} = 3.91$, $g_{*,rh} = 106.75$, and $T_0 = 2.35 \times 10^{-4}$ eV, finally we can get

$$r_{FS} \simeq 2.8 \times 10^{-2} \left(\frac{\mathrm{keV}}{m_\chi} \right) \left(\frac{50}{K} \right)^{\frac{1}{2}}$$
$$\times \left(1 + 0.09 \ln \left[\left(\frac{m_\chi}{\mathrm{keV}} \right) \left(\frac{K}{50} \right)^{\frac{1}{2}} \right] \right) \mathrm{Mpc}. \quad (45)$$

The most stringent bound on r_{FS} comes from small structure formation $r_{FS} < 0.1$ Mpc [63]. The relationship between the mass of χ and its free-streaming length is depicted in Fig. 4. Basically speaking, warm DM is obtained for $m_\chi \sim 10$ keV while $K \in [0.01, 100]$.

Meanwhile, χ becomes cold DM when χ is sufficiently heavy and/or the decay parameter K is large enough.

V. COMBINED ANALYSIS

After studying some benchmark points, it would be better to figure out the viable parameter space for successful leptogenesis and DM. We then perform a random scan over the following parameter space:
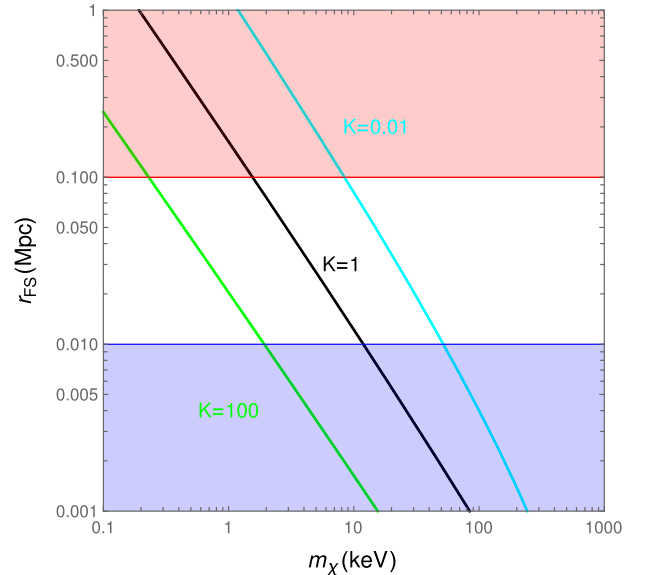

FIG. 4.   Influence of free streaming on DM mass. The red area ($r_{FS} > 0.1$ Mpc), white area (0.1 Mpc $> r_{FS} > 0.01$ Mpc), and blue area ($r_{FS} < 0.01$ Mpc) correspond to the hot, warm, and cold DM scenario [64], respectively.
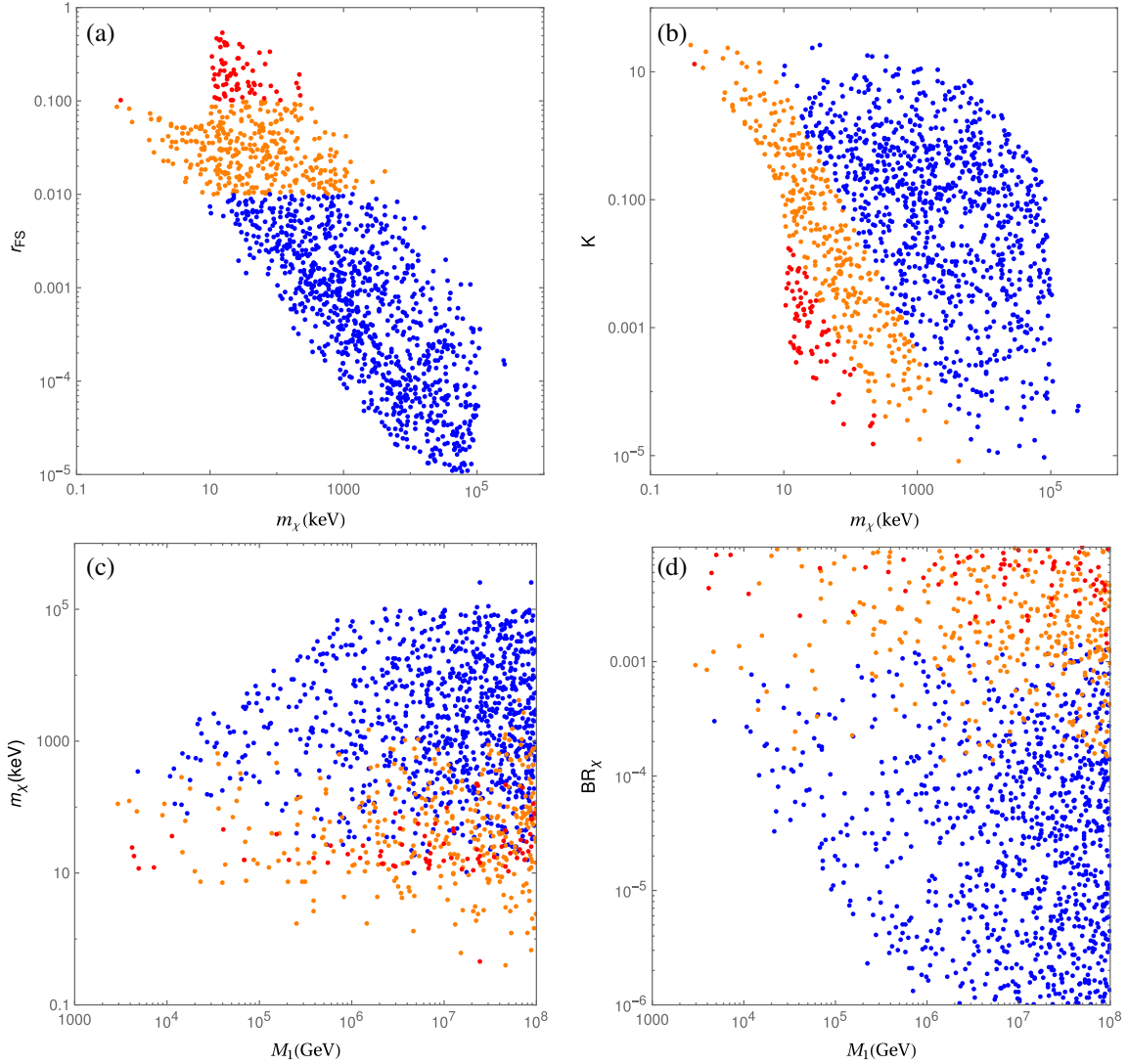
FIG. 5. Viable parameter space for DM. The red, orange, and blue points correspond to hot, warm, and cold DM, respectively.

$$m_1 \in [10^{-12}, 10^{-2}] \text{ eV}, \qquad M_1 \in [10^3, 10^8] \text{ GeV},$$

$$v_\nu \in [10^{-2}, 10^2] \text{ GeV},$$

$$\text{Re}(\omega_{12,13,23}) \in [10^{-10}, 1], \qquad \text{Im}(\omega_{12,13,23}) \in [10^{-10}, 1],$$

$$\text{BR}_\chi \in [10^{-6}, 10^{-2}]. \tag{46}$$

During the scan, we have fixed $M_2/M_1 = M_3/M_2 = 10$. The final obtained baryon asymmetry $Y_{\Delta B}$ is required to be within 3σ ranges of the observed value, i.e., $Y_{\Delta B} \in [8.60, 8.84] \times 10^{-11}$. The results are shown in Figs. 5 and 6 for DM and leptogenesis, respectively.

Let us consider the DM results in Fig. 5 first. According to the dominant constraint from free-streaming length r_{FS}, we can divide viable samples into three scenarios in Fig. 5(a). Of course, the hot DM scenario is not favored by small structure formation. For warm DM, $m_\chi \in [0.3, 2 \times 10^3]$ keV is possible. Meanwhile for cold DM,

$m_\chi \in [10, 2 \times 10^5]$ keV is allowed. And r_{FS} is down to about 10^{-5} Mpc when $m_\chi \sim 10^5$ keV. From Fig. 5(b), we are aware that the hot DM samples correspond to those with small DM mass m_χ and very weak washout effect $K \lesssim 10^{-2}$. Figure 5(c) shows the samples in the $m_\chi - M_1$ plane. Three kinds of DM are all possible for a certain value of M_1. By the way, it is interesting to obtain an upper limit on m_χ when $M_1 \lesssim 10^6$ GeV. This indicates that for TeV-scale leptogenesis, FIMP DM should be keV to sub-MeV. The result for BR_χ is shown in Fig. 5(d), which tells us that warm DM requires $\text{BR}_\chi \gtrsim 10^{-4}$ and cold DM requires $\text{BR}_\chi \lesssim 10^{-3}$, respectively.

Then, we consider the leptogenesis results in Fig. 6. The generalized Davidson-Ibarra bound is clearly seen in Fig. 6(a). The (warm and cold DM) allowed samples show that the mass of N_1 for successful leptogenesis could be down to about 3 TeV. The viable region of the $v_\nu - M_1$
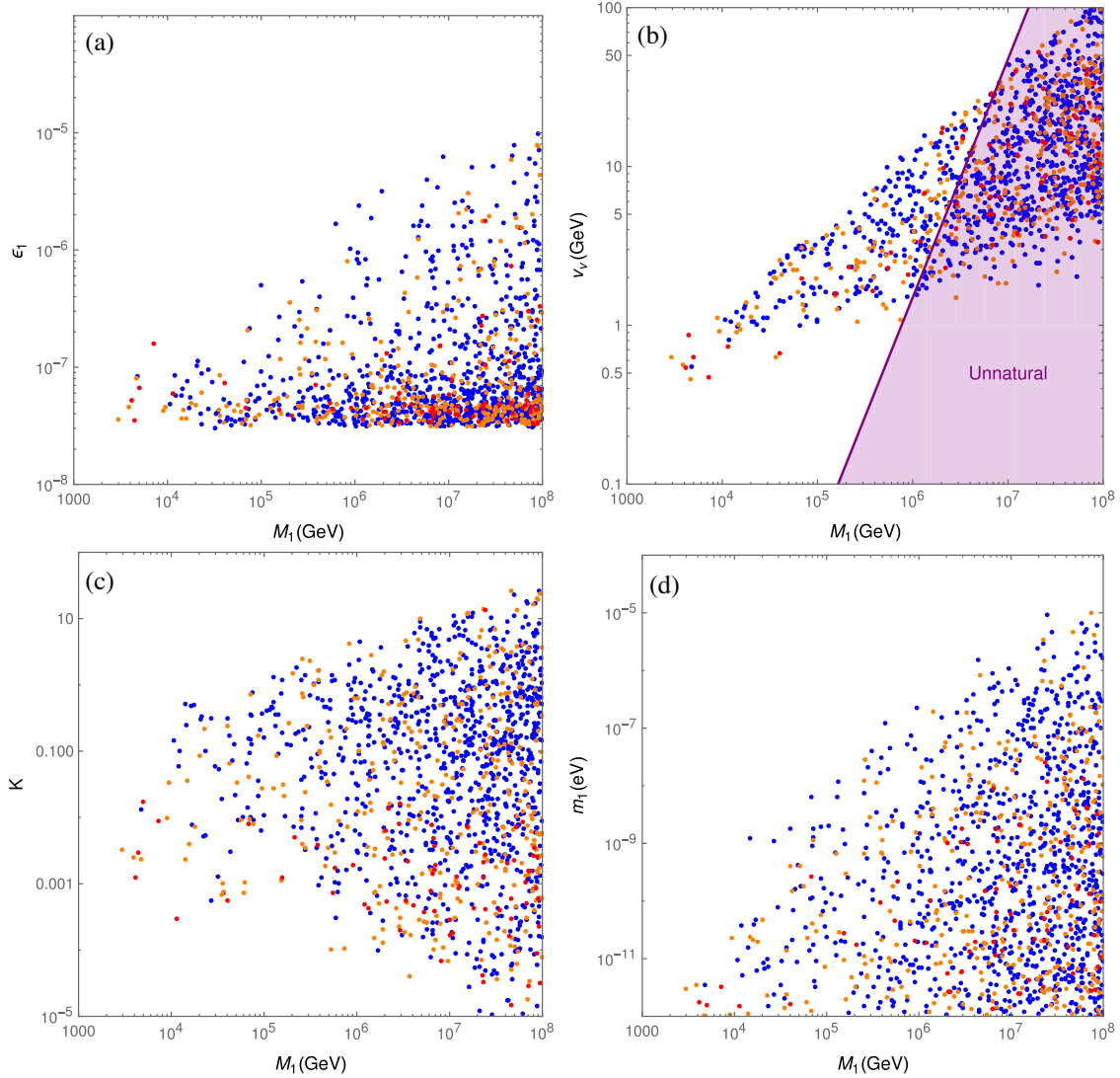
FIG. 6.   Same as Fig. 5, but for leptogenesis.

plane is shown in Fig. 6(b), which is consistent with the theoretical bounds discussed in Ref. [17]. For completeness, the naturalness bound in Eq. (4) is also shown. Therefore, natural leptogenesis is viable for 3×10^3 GeV $\lesssim M_1 \lesssim 7 \times 10^6$ GeV with 0.4 GeV $\lesssim v_\nu \lesssim 30$ GeV. The result for decay parameter K is given in Fig. 6(c), which shows that $K \lesssim 10$ should be satisfied when $M_1 \lesssim 10^8$ GeV. Actually, for $M_1 \lesssim 10^5$ GeV, all the samples are within the weak washout region. An upper bound on lightest neutrino mass m_1 is clearly seen in Fig. 6(d). It also indicates that successful leptogenesis in the ν2HDM requires that m_1 must be extremely tiny, e.g., $m_1 \lesssim 10^{-11}$ eV for $M_1 \sim 10^4$ GeV.

Before ending this section, we give a brief discussion on the collider signature. According to the results of leptogenesis in Fig. 6, not too small v_ν is favored. In such a scenario, the branching ratios of neutrinophilic scalars are quite different from the scenario with small v_ν [45,65–67], but are similar to type-I 2HDM [68]. Currently, if m_{Φ_ν} is

smaller than m_t, the most stringent constraint comes from $t \to bH^\pm(H^\pm \to \tau^\pm \nu)$ [69], which could exclude the region $v_\nu \gtrsim 18$ GeV [70]. Meanwhile, if $m_Z + m_h \lesssim m_{\phi_\nu} \lesssim 2m_t$, the channel $A \to Zh(h \to b\bar{b})$ could exclude the region $v_\nu \gtrsim 24$ GeV [71]. For heavier additional scalars with $m_{\Phi_\nu} > 2m_t$, the signature $A/H \to t\bar{t}$ is only able to probe the region $v_\nu \gtrsim 174$ GeV [72,73]. Therefore, the experimental bounds on neutrinophilic scalars can be easily escaped providing m_{Φ_ν} is large enough. At the HL LHC, the signature $A \to Zh(h \to b\bar{b})$ would reach $v_\nu \sim 10$ GeV [73]. Then the observation of this signature will indicate $M_1 \sim 10^6$ GeV and $m_1 \lesssim 10^{-7}$ eV.

VI. CONCLUSION

In this paper, we propose an extended ν2HDM to interpret the neutrino mass, leptogenesis, and dark matter simultaneously. This model contains one neutrinophilic

scalar doublet Φ_ν, three right-hand heavy neutrinos N, which account for low scale neutrino mass generation similar to the type-I seesaw mechanism. Leptogenesis is generated due to the CP-violating decays of right-hand neutrino $N \rightarrow \ell_L \Phi_\nu^*$, $\bar{\ell}_L \Phi_\nu$. The dark sector contains one scalar singlet ϕ and one Dirac fermion singlet χ, which are charged under a Z_2 symmetry. Provided $m_\chi < m_\phi$ and $\lambda \ll 1$, χ is a FIMP DM candidate within this paper. The relic abundance of χ is produced by $N \rightarrow \chi\phi$. Therefore, we have a common origin, i.e., the heavy right-hand neutrinos N, for tiny neutrino mass, baryon asymmetry, and dark matter.

In the framework of ν2HDM, the asymmetry ϵ_1 and decay parameter K are both enhanced by the smallness of v_ν. By explicit calculation, we show that the decay parameter K can be suppressed under certain circumstances. And a hierarchical structure of Yukawa coupling y is needed to induce leptogenesis at low scale for the nondegenerate mass of N. The importance of the $\Delta L = 2$ washout process is also illustrated. As for FIMP DM, the relic abundance mainly depends on the branching ratio BR_χ and decay parameter K, and m_χ is typically at the order of keV to MeV scale. Meanwhile, the free-streaming length sets a stringent bound. The viable parameter space for successful leptogenesis and DM is obtained by solving the corresponding Boltzmann equations. To keep this model natural, we find $10^3 \text{ GeV} \lesssim M_1 \lesssim 10^6 \text{ GeV}$, $0.4 \text{ GeV} \lesssim v_\nu \lesssim 30 \text{ GeV}$, $m_1 \lesssim 10^{-5} \text{ eV}$, and $K \lesssim 10$ is favored by leptogenesis. Meanwhile, the warm (cold) DM mass in the range $m_\chi \in [0.3, 2 \times 10^3] \text{ keV}$ ($m_\chi \in [10, 2 \times 10^5] \text{ keV}$) is predicted with $\mathrm{BR}_\chi \gtrsim 10^{-4}$ ($\mathrm{BR}_\chi \lesssim 10^{-3}$).

ACKNOWLEDGMENTS

[1] Y. Fukuda *et al.* (Super-Kamiokande Collaboration), Phys. Rev. Lett. **81**, 1562 (1998).

[2] Q. R. Ahmad *et al.* (SNO Collaboration), Phys. Rev. Lett. **89**, 011301 (2002).

[3] P. Minkowski, Phys. Lett. **67B**, 421 (1977).

[4] R. N. Mohapatra and G. Senjanovic, Phys. Rev. Lett. **44**, 912 (1980).

[5] M. Fukugita and T. Yanagida, Phys. Lett. B **174**, 45 (1986).

[6] S. Davidson and A. Ibarra, Phys. Lett. B **535**, 25 (2002).

[7] F. Vissani, Phys. Rev. D **57**, 7027 (1998).

[8] J. D. Clarke, R. Foot, and R. R. Volkas, Phys. Rev. D **91**, 073009 (2015).

[9] A. Pilaftsis and T. E. J. Underwood, Nucl. Phys. **B692**, 303 (2004).

[10] E. K. Akhmedov, V. A. Rubakov, and A. Y. Smirnov, Phys. Rev. Lett. **81**, 1359 (1998).

[11] T. Asaka and M. Shaposhnikov, Phys. Lett. B **620**, 17 (2005).

[12] T. Hambye and D. Teresi, Phys. Rev. Lett. **117**, 091801 (2016).

[13] T. Hambye and D. Teresi, Phys. Rev. D **96**, 015031 (2017).

[14] S. Baumholzer, V. Brdar, and P. Schwaller, J. High Energy Phys. 08 (2018) 067.

[15] T. Alanne, T. Hugle, M. Platscher, and K. Schmitz, J. Cosmol. Astropart. Phys. 03 (**2019**) 037.

[16] W. Chao and M. J. Ramsey-Musolf, Phys. Rev. D **89**, 033007 (2014).

[17] J. D. Clarke, R. Foot, and R. R. Volkas, Phys. Rev. D **92**, 033006 (2015).

[18] E. Ma, Mod. Phys. Lett. A **21**, 1777 (2006).

[19] T. Hambye, F. Ling, L. Lopez Honorez, and J. Rocher, J. High Energy Phys. 07 (**2009**) 090.

[20] S. Kashiwase and D. Suematsu, Phys. Rev. D **86**, 053001 (2012).

[21] S. Kashiwase and D. Suematsu, Eur. Phys. J. C **73**, 2484 (2013).

[22] J. Racker, J. Cosmol. Astropart. Phys. 03 (2014) 025.

[23] T. Hugle, M. Platscher, and K. Schmitz, Phys. Rev. D **98**, 023020 (2018).

[24] D. Borah, A. Dasgupta, and S. K. Kang, arXiv:1806.04689.

[25] D. Borah, P. S. B. Dev, and A. Kumar, Phys. Rev. D **99**, 055012 (2019).

[26] D. Mahanta and D. Borah, J. Cosmol. Astropart. Phys. 04 (2020) 032.

[27] E. Ma, Phys. Rev. Lett. **86**, 2502 (2001).

[28] N. Haba and O. Seto, Prog. Theor. Phys. **125**, 1155 (2011).

[29] N. Haba and O. Seto, Phys. Rev. D **84**, 103524 (2011).

[30] S. Dodelson and L. M. Widrow, Phys. Rev. Lett. **72**, 17 (1994).

[31] M. Drewes *et al.*, J. Cosmol. Astropart. Phys. 01 (2017) 025.

[32] A. Adulpravitchai and M. A. Schmidt, J. High Energy Phys. 12 (2015) 023.

[33] Z. L. Han, B. Zhu, L. Bian, and R. Ding, arXiv:1812.00637.

[34] A. Boyarsky, M. Drewes, T. Lasserre, S. Mertens, and O. Ruchayskiy, Prog. Part. Nucl. Phys. **104**, 1 (2019).

[35] S. Antusch, P. Di Bari, D. A. Jones, and S. F. King, Phys. Rev. D **86**, 023516 (2012).

[36] D. Mahanta and D. Borah, J. Cosmol. Astropart. Phys. 11 (2019) 021.

[37] M. Chianese and S. F. King, J. Cosmol. Astropart. Phys. 09 (2018) 027.

[38] M. Chianese, B. Fu, and S. F. King, J. Cosmol. Astropart. Phys. 03 (2020) 030.

[39] E. Aprile *et al.* (XENON Collaboration), Phys. Rev. Lett. **121**, 111302 (2018).

[40] M. Ackermann *et al.* (Fermi-LAT Collaboration), Phys. Rev. Lett. **115**, 231301 (2015).

[41] N. Bernal, M. Heikinheimo, T. Tenkanen, K. Tuominen, and V. Vaskonen, Int. J. Mod. Phys. A **32**, 1730023 (2017).

[42] S. M. Davidson and H. E. Logan, Phys. Rev. D **80**, 095008 (2009).

[43] T. Morozumi, H. Takata, and K. Tamai, Phys. Rev. D **85**, 055002 (2012); **89**, 079901(E) (2014).

[44] N. Haba and T. Horita, Phys. Lett. B **705**, 98 (2011).

[45] C. Guo, S. Y. Guo, Z. L. Han, B. Li, and Y. Liao, J. High Energy Phys. 04 (2017) 065.

[46] G. Aad *et al.* (ATLAS Collaboration), Phys. Lett. B **716**, 1 (2012).

[47] S. Chatrchyan *et al.* (CMS Collaboration), Phys. Lett. B **716**, 30 (2012).

[48] P. A. N. Machado, Y. F. Perez, O. Sumensari, Z. Tabrizi, and R. Z. Funchal, J. High Energy Phys. 12 (2015) 160.

[49] J. A. Casas and A. Ibarra, Nucl. Phys. **B618**, 171 (2001).

[50] A. Ibarra and G. G. Ross, Phys. Lett. B **591**, 285 (2004).

[51] E. Nardi, Y. Nir, E. Roulet, and J. Racker, J. High Energy Phys. 01 (2006) 164.

[52] S. Davidson, E. Nardi, and Y. Nir, Phys. Rep. **466**, 105 (2008).

[53] N. Aghanim *et al.* (Planck Collaboration), arXiv:1807 .06209.

[54] W. Wang and Z. L. Han, J. High Energy Phys. 04 (2017) 166.

[55] A. Falkowski, J. T. Ruderman, and T. Volansky, J. High Energy Phys. 05 (2011) 106.

[56] A. Falkowski, E. Kuflik, N. Levi, and T. Volansky, Phys. Rev. D **99**, 015022 (2019).

[57] W. Buchmuller, P. Di Bari, and M. Plumacher, Ann. Phys. (Amsterdam) **315**, 305 (2005).

[58] I. Esteban, M. C. Gonzalez-Garcia, A. Hernandez-Cabezudo, M. Maltoni, and T. Schwetz, J. High Energy Phys. 01 (2019) 106.

[59] J. A. Harvey and M. S. Turner, Phys. Rev. D **42**, 3344 (1990).

[60] L. J. Hall, K. Jedamzik, J. March-Russell, and S. M. West, J. High Energy Phys. 03 (2010) 080.

[61] M. Tanabashi *et al.* (Particle Data Group), Phys. Rev. D **98**, 030001 (2018).

[62] P. A. R. Ade *et al.* (Planck Collaboration), Astron. Astrophys. **594**, A13 (2016).

[63] A. Berlin and N. Blinov, Phys. Rev. Lett. **120**, 021801 (2018).

[64] A. Merle, V. Niro, and D. Schmidt, J. Cosmol. Astropart. Phys. 03 (2014) 028.

[65] N. Haba and K. Tsumura, J. High Energy Phys. 06 (2011) 068.

[66] W. Wang and Z. L. Han, Phys. Rev. D **94**, 053015 (2016).

[67] K. Huitu, T. J. Karkkainen, S. Mondal, and S. K. Rai, Phys. Rev. D **97**, 035026 (2018).

[68] G. C. Branco, P. M. Ferreira, L. Lavoura, M. N. Rebelo, M. Sher, and J. P. Silva, Phys. Rep. **516**, 1 (2012).

[69] A. M. Sirunyan *et al.* (CMS Collaboration), J. High Energy Phys. 07 (2019) 142.

[70] P. Sanyal, Eur. Phys. J. C **79**, 913 (2019).

[71] M. Aaboud *et al.* (ATLAS Collaboration), J. High Energy Phys. 03 (2018) 174; 11 (2018) 051(E).

[72] M. Aaboud *et al.* (ATLAS Collaboration), Phys. Rev. Lett. **119**, 191803 (2017).

[73] N. Chen, T. Han, S. Li, S. Su, W. Su, and Y. Wu, arXiv: 1912.01431.